TEST OF THE IMAGING PROPERTIES OF INORGANIC SCINTILLATION SCREENS USING FAST AND SLOW EXTRACTED ION BEAMS*

A. Lieberwirth[1,2,3], W. Ensinger[2], P. Forck[1,3,#], O. Kester [1,3], S. Lederer[1,2], T. Sieber[1],
B. Walasek-Höhne[1], GSI Helmholtz-Zentrum für Schwerionenforschung, Darmstadt, Germany
also at [2] Technical University Darmstadt, Institute for Material Science, Germany
also at [3] University Frankfurt, Institute of Applied Physics, Germany

Abstract

Inorganic scintillation screens (phosphor P43 and P46, single crystal YAG:Ce, ceramic Alumina and Chromium-doped Alumina), as used for transverse profile determination, were investigated concerning light output, profile reproduction and spectral emission. The screens were irradiated with ion pulses extracted from the synchrotron SIS18 at 300 MeV/u and intensities from about 10^6 to 10^{10} particles per pulse using either 1 µs fast extraction or $\approx$ 300 ms slow extraction. The light output coincides for both extraction modes. For all materials the optical emission spectrum is independent on the ion species and beam intensities. Radiation hardness tests were performed with up to 10^{12} accumulated Nickel: The phosphor P46 and single crystal YAG:Ce show no significant decrease of light output, while for P43 and Chromox a decrease by 5 to 15 % was measured.

OVERVIEW OF INVESTIGATIONS

Intersecting scintillation screens determine two dimensional beam images and are frequently used for transverse profile measurements in beam transfer lines [1]. The following properties have been investigated:

- emission characteristics for different ion species (p, N, Ni, Xe, U) with a kinetic energy of 300 MeV/u
- dynamic range and linearity between the incident particle intensities and the light output within a range of 10^6 to 10^{10} particles per pulse (ppp)
- spectral emission for various ions and intensities
- radiation hardness i.e. possible variation of the emission characteristics as a function of fluence.

As scintillators we investigated phosphor screens P43 and P46 consisting of crystalline powder with a typical gain size of 10 µm, two different single crystal YAG:Ce and ceramics disks made of pure Alumina A999 (99.99 % purity) and Chromium-doped Alumina (Cr with 0.04 % weight), the properties are compiled in Table 1. All screens were irradiated in air.

The ion beams were extracted from the synchrotron SIS18 at GSI with intensities varying from $6 \cdot 10^6$ ppp up to $2 \cdot 10^{10}$ ppp. The pulse duration was 300–400 ms for slow and 1 µs for fast, single turn extraction at a general requested kinetic energy of 300 MeV/u. One standard deviation of the beam profile was typically $\sigma \approx 3$ mm.

A resonant transformer was used to measure the current of the fast extracted beam with an accuracy of 15% [2]. For intensity measurements in slow extraction mode a detector was used, that consists of an Ionization Chamber (6.5 mm 80 % Ar +20 % CO_2 gas mixture, separated by two 100 µm stainless steel walls from the vacuum, measurement accuracy: 15%) and a SEM (three 100 µm Al plates, measurement accuracy: 15%) [3]. Additionally, the beam passed a 50 µm thick stainless steel foil to air 72 cm before the target ladder. Thus the beam was stripped and the kinetic energies at the target surface were calculated numerically by the code LISE [4] as summarized in Table 2.

Table 1: Investigated Scintillation Screens, ∅ 5 to 8 cm

Name	Material	Thick.	Supplier
#1 P43	Gd_2O_2S:Tb	50 µm	ProxiVision
#2 P46	$Y_3Al_5O_{12}$:Ce	50 µm	ProxiVision
#3 P46	$Y_3Al_5O_{12}$:Ce	20 µm	Crytur
#4 YAG:Ce	$Y_3Al_5O_{12}$:Ce	250 µm	Crytur
#5 YAG:Ce	$Y_3Al_5O_{12}$:Ce	1 mm	SaintGobian
#6 Alumina	Al_2O_3	800 µm	BCE
#7 Chromox	Al_2O_3:Cr	800 µm	BCE

Table 2: The Beam Kinetic Energy E in Front of the Target

Projectile	Slow extr. E [MeV/u]	Fast extr. E [MeV/u]
Proton $^{1}_{1}$H	299.2	299.8
Nitrogen $^{14}_{7}$N	297	299
Nickel $^{58}_{28}$Ni	298	297
Xenon $^{124}_{54}$Xe	281	295
Uranium $^{238}_{92}$U	272	292

OPTICAL SETUP AND ANALYSIS

The scintillation screens on the target ladder were mounted with 45° orientation with respect to the beam plane with an optical setup mounted perpendicular to the target surface as shown in Fig. 1. It consists of two types of cameras (blue in Fig. 1):

Camera #1: AVT Marlin or Stingray, 1/2" CCD chip, 8 bit resolution, monochrome, mounted with a distance of 50 cm with respect to the targets slightly below the optic axis and recorded the two dimensional response of the scintillation screen. The camera was equipped with a Pentax C1614ER lens of 16 mm focal length and remote-

ly controlled iris. The spectral transmittance ranges from 360 to 1000 nm [5]. To further increase the dynamic range of the measurements a neutral-density-filter (Hoya ND03, 5% transmission) could be mounted additionally. The recorded images served for investigations in light output L and the beam profiles.

Camera #2: PCO 1600, 12.2 mm x 9.0 mm CCD sensor size, 14 bit resolution, monochrome, mounted on a Horiba CP140-202 spectrometer with an average dispersion of 50 nm/mm [6] and a wavelength range from 230 to 800 nm. A Pentax C2514-M lens of 25 mm focal length [5] with a wavelength range from 360 to 1000 nm was used. It was focused on an adjustable slit, mounted in horizontal orientation on the input of the spectrometer. To increase the light input the slit was opened until a wavelength resolution of 8.5 nm FWHM was reached. The distance to the target was about 70 cm.

Images were recorded simultaneously from both cameras during irradiation. Background images were recorded shortly before incoming pulses and subtracted from the beam images. The spectra obtained by camera #2 were folded with the transmission efficiency of the optical system.

In the following the term light output L refers to the light recorded by camera #1. The term light yield Y describes the light output normalized to the energy loss ΔE per single ion in the scintillation material and to the delivered particles per pulse as $Y = L/(\Delta E \cdot ppp)$; ΔE is calculated using the LISE code [4] .

ed particles per pulse. In the investigated ranges of $3 \cdot 10^6$ till $2 \cdot 10^8$ ppp all investigated materials respond linear to the number of irradiated particles per pulse i.e. no saturation effect was observed. From the investigated phosphor screens the highest light output is observed from the P43 material. Only YAG:Ce (Saint Gobain) showed an even higher light output. It is supposed that the screen thickness of 1 mm and the resulting large energy deposition is responsible for this observation. The lowest light output is observed from pure Aluminum Oxide. Chrome-doping induces here a factor of ≈ 5 more light. Investigations in slow extraction mode show similar results. Comparable data with other ion beam parameter were reported earlier [7-11].
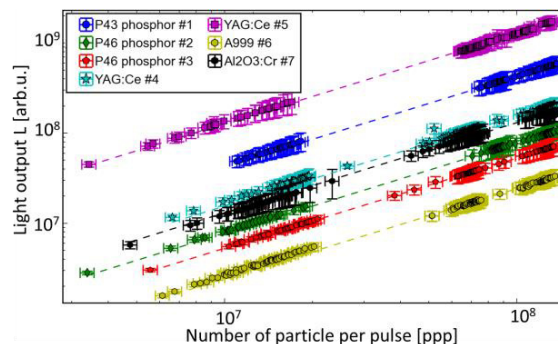
Figure 2: Light output L of all investigated targets under irradiation with a fast extracted Uranium beam as function of irradiating particles per pulse.
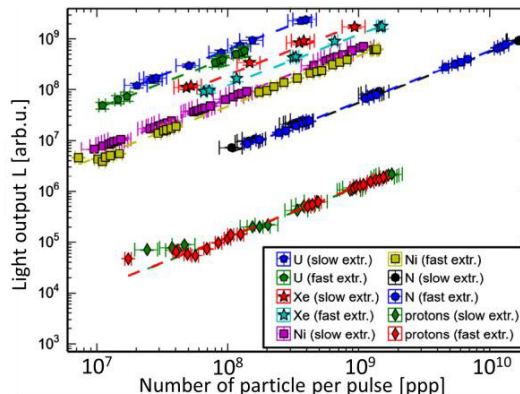
Figure 3: Light output L of the P43 phosphor screen induced by various projectiles as function of the number of irradiating particles per pulse for slow and fast extraction.

Figure 3 shows the light output of the material P43 phosphor for fast and slow extraction for several ions. For better visibility only each 15th data point is plotted with errors between 5% and 25% concerning L and 15% concerning the number of irradiated particles per pulse in both extraction modes. All ions were accelerated to the same energy per nucleon; the actual beam energies are summarized in Table 2. As can be seen, protons induce the lowest light output and for increasing atomic number of the projectile the slope increases up to the light output induced by Uranium ions.
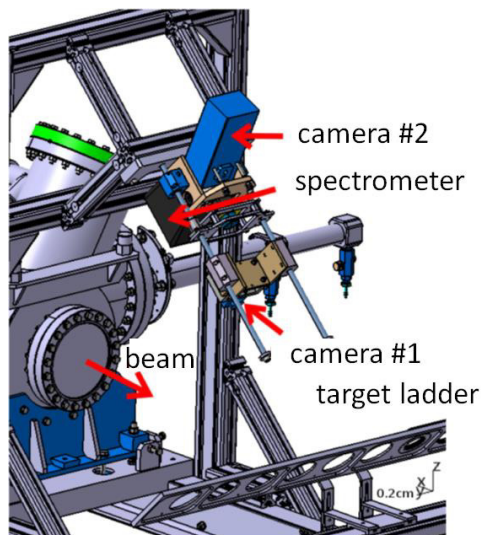

Figure 1: Scheme of the experimental setup. The distance between the air window and the target ladder is 72 cm.

LIGHT OUTPUT AND YIELD

As an example for the light output L the comparison for all investigated scintillation screens under irradiation of fast extracted Uranium beam is depicted in Fig. 2. The errors bars are between 5% and 20% concerning L, as originated by the signal-to-noise-ratio in the recorded images and 15% error concerning the number of irradiat-

To summarize those findings, the relative light yield was calculated and normalized to the yield from Nitrogen for each scintillation screen individually. Figure 4 depicts the results for the investigated ions as a function of the stopping power *dE/dx* in the scintillation material. For all materials the light yield decreases for heavier projectiles, however the ratio of light yields for protons to Uranium differs for all screen materials by a factor less than 5. This coincides with previous finding [11]. Within the error bars, the behavior is independent on the beam delivery time (1 µs or 300 ms), i.e. there is no time dependent saturation effect for the given beam intensities.
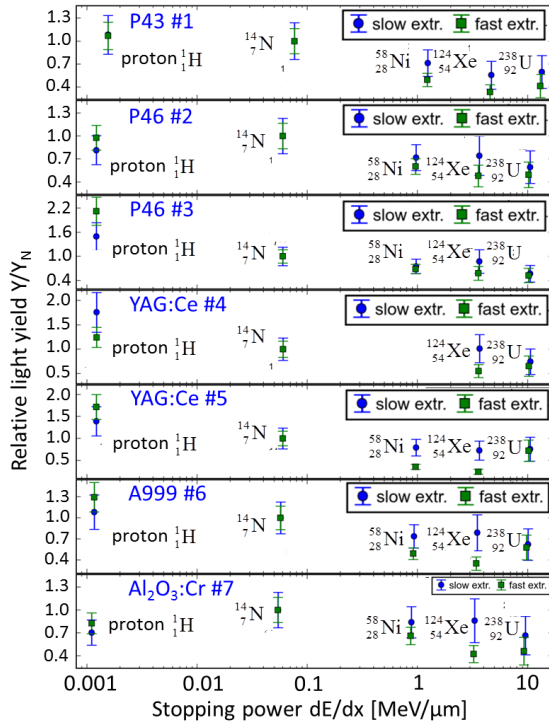

Figure 4: Relative light yield *Y* of all scintillators in dependence of the stopping power *dE/dx* of the investigated projectiles for slow and fast extraction mode.
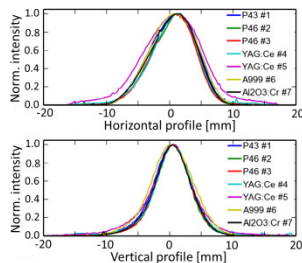

Figure 5: Horizontal and vertical beam profiles obtained from the scintillation screens under irradiation with a fast extracted Xenon beam at 10^9 ppp.

PROFILE REPRODUCTION

From the recorded images the beam profiles were calculated by projection in horizontal and vertical direction. Figure 5 shows a comparison of beam profiles from the investigated scintillators during irradiation with fast extracted Xenon beam. The phosphor and ceramic screens

as well as single crystal YAG:Ce #4 show the same projections, i.e. the beam properties are well reproduced. In case of the single crystal YAG:Ce #5 the beam appears broader in horizontal direction only, which is most likely assigned to the 1 mm thickness of the target and the increased scattering in the screen.

RADIATION HARDNESS TEST

Investigations concerning possible degradation of the scintillation efficiency for Nickel ions very performed. Figure 6 depicts the irradiation by about 1100 pulses of Nickel ions with typically $2 \cdot 10^9$ ppp. The irradiation was stopped for 15 min and then continued by 100–150 pulses to check for any permanent modification of the materials.
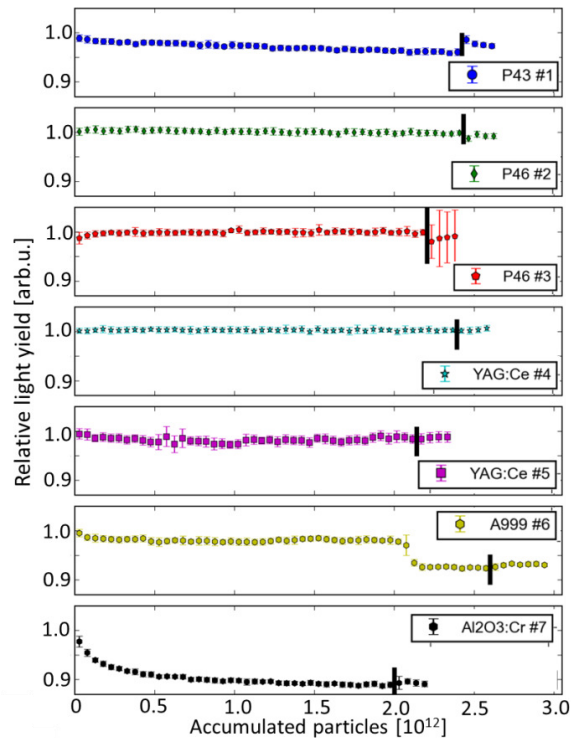

Figure 6: Light yield as a function of accumulated Nickel ions of ≈1100 pulses with $2 \cdot 10^9$ ppp. For better visibility the data points of 20 pulses are binned. The black bar indicates a break of irradiation of 15 min.

The data points in Fig. 6 were binned to a beam intensity of ≈$5 \cdot 10^{10}$ (20 points), statistical deviations of the single pulses are used as error bars. A decrease of less than 5% is observed for P43 phosphor after a deposit of $2 \cdot 10^{12}$ ions. P43 starts from the initial value of light yield after the 15 min break, but the yield decreases with a considerable slope. Single crystal YAG:Ce and the corresponding phosphor P46 were found to be stable. A larger decrease was found for Al_2O_3:Cr with 10% loss of light yield.

Figure 7 shows the corresponding beam widths as characterized by the second statistical moment σ_{hor} and $\sigma_{vert.}$ Sudden steps of the beam size during irradiation of Alumina and during the breaks are caused by beam instabilities. During the permanent irradiation six screens show

constant beam sizes, only YAG:Ce #5 shows a systematic image degeneration. The recorded beam size is unchanged after the irradiation break for the three targets, P43 #1, P46 #2 and YAG:Ce #4.
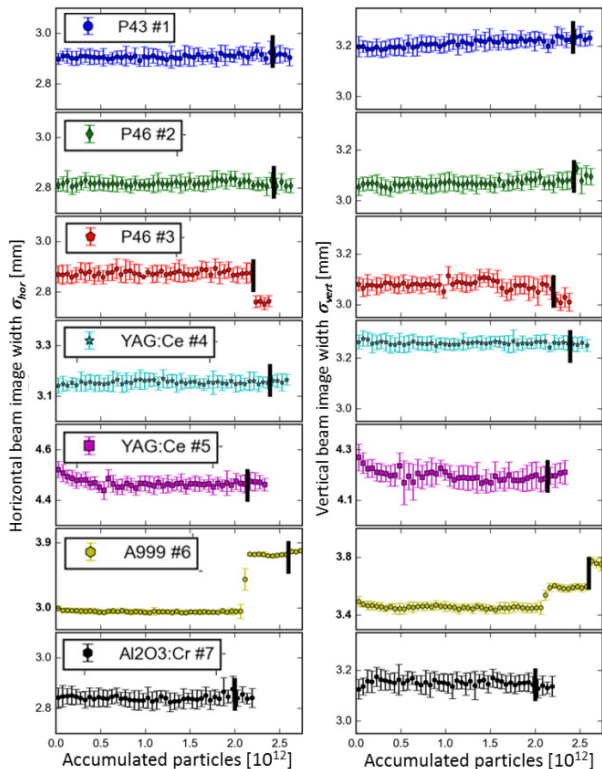

Figure 7: Horizontal and vertical standard deviation of the profiles with the same parameters as in Fig. 6.
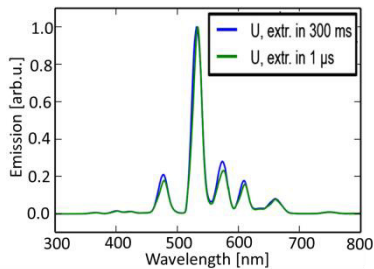

Figure 8: Emission spectra of P43 for Uranium of 10^9 ppp for fast and slow extraction mode.

EMSSION SPECTRA

An example of the emission spectrum of P43 under Uranium irradiation is shown in Fig. 8 averaged over the 10^8 till 10^9 ppp irradiation campaign. The spectra for both extraction modes show the same characteristics, which was also the case for all other ion species. Moreover, the spectrum is comparable to the one obtained by electron or x-ray irradiation [12], which was unexpected due to the significantly higher energy deposition from a single ion compared to an electron or photon. In general, for all screen materials, projectiles and extraction modes no modification of the emission spectra was recorded during the radiation hardness tests [7].

CONCLUSION

Detailed tests of several inorganic scintillation screens were performed for 300 MeV/u ions. For the same beam conditions but different screens the light output varies by about a factor of 100. For low and medium intensities no saturation of the light output were recorded providing a large dynamic range for profile determination. Within the experimental uncertainties, similar light output levels were achieved independent on the extraction time, which was chosen quite differently to be 1 µs and some 100 ms, respectively. Correspondingly, no saturation was observed even for heavy ions with large energy deposition and a beam delivery comparable to the luminescence lifetime of some materials. The ratio of the light yield, i.e. the amount of photons per single particle energy loss, decreases from protons to Uranium by a factor of two to five for the various materials. The radiation hardness test proves the stability in particular for single crystal YAG:Ce #4 and the corresponding phosphors P46 #2 and #3. The beam profiles are well reproduced by these materials. Chromox suffers from a decrease of light yield as a function of fluence, but the beam profile is still well reproduced. The optical emission spectra depend neither on the irradiating ion (despite large differences in energy deposition) nor on the extraction time and is comparable to the one obtained from electron or x-ray irradiation. The emission spectra remain unchanged even after deposition of some 10^{12} ions. Further results are published elsewhere [7-11].

Among the investigated materials YAG:Ce #4 and P46 will be a good choice for the installation at the High Energy Beam Transport lines at FAIR usable for low and medium intensities.

REFERENCES

[1] B. Walasek-Höhne, G. Kube, in *Proc. DIPAC 2011*, Hamburg, Germany, p. 533 (2011).

[2] H. Reeg, N. Schneider, in *Proc. DIPAC 2001*, Grenoble, France, p.120 (2001).

[3] P. Forck, T. Hoffmann, A. Peters, in *Proc. DIPAC 1997*, Frascati, Italy, p. 165 (1997).

[4] O.B. Tarasov, D. Bazin etal., LISE++, http://lise.nscl.msu.edu/lise.html

[5] Pentax C1614ER HR and C2514-M Specification

[6] HORIBA, www.horiba.com

[7] A. Lieberwirth *et al.*, Nucl. Instrum. Meth. B **365**, 533 (2015).

[8] P. Forck *et al.*, in *Proc. IPAC 2014*, Dresden, Germany, p. 3480 (2014).

[9] A. Lieberwirth *et al.*, in *Proc. IBIC 2013*, Oxfors, UK, p. 553 (2013).

[10] K. Renuka *et al.*, in *Proc. BIW 2012*, Newport News, USA, p. 183 (2012).

[11] K. Renuka *et al.*, IEEE Trans. Nucl. Sc. **59**, p. 2301, dx.doi.org/10.1109/TNS.2012.2197417 (2012).

[12] E. Gorokhova *et al.*, IEEE Trans. Nucl. Sci. **52**, 3129 dx.doi.org/10.1109/TNS.2005.862827 (2005).